The Astrophysical Journal, 646:886–898, 2006 August 1

PHASE-SPACE DISTRIBUTIONS OF CHEMICAL ABUNDANCES IN MILKY WAY–TYPE GALAXY HALOS

Andreea S. Font,[1] Kathryn V. Johnston,[1] James S. Bullock,[2] and Brant E. Robertson[3]

Received 2005 December 26; accepted 2006 April 16

ABSTRACT

Motivated by upcoming data from astrometric and spectroscopic surveys of the Galaxy, we explore the chemical abundance properties and phase-space distributions in hierarchically formed stellar halo simulations set in a ΛCDM universe. Our stellar halo metallicities increase with stellar halo mass. The slope of the [Fe/H]-M_* trend mimics that of the satellite galaxies that were destroyed to build the halos, implying that the relation propagates hierarchically. All simulated halos contain a significant fraction of old stellar populations accreted more than 10 Gyr ago, and in a few cases some intermediate-age populations exist. In contrast with the Milky Way, many of our simulated stellar halos contain old stellar populations that are metal-rich, originating in the early accretion of massive satellites ($M_* \sim 10^9\ M_\odot$). We suggest that the (metal-rich) stellar halo of M31 falls into this category, while the more metal-poor halo of the Milky Way is lacking in early massive accretion events. Interestingly, our hierarchically formed stellar halos often have nonnegligible metallicity gradients in both [Fe/H] and [α/Fe]. These gradients extend a few tens of kiloparsecs, and can be as large as 0.5 dex in [Fe/H] and 0.2 dex in [α/Fe], with the most metal-poor halo stars typically buried within the central ~5 kpc of the galaxy. Finally, we find that chemical abundances can act as a rough substitute for time of accretion of satellite galaxies, and, based on this finding, we propose a criterion for identifying tidal streams spatially by selecting stars with [α/Fe] ratios below solar.

Subject headings: cosmology: theory — galaxies: abundances — galaxies: evolution

1. INTRODUCTION

The stars in the halo hold important information about the formation history of the Galaxy. Their spatial and velocity distributions can be used to retrace their dynamic origin, and their chemical abundances can constrain the star formation histories of their constituents. A major goal over the next decade is to obtain kinematic and chemical information for a large number of stars in our own Galaxy, thus providing a detailed reconstruction of its formation history and a link to the underlying cosmology (e.g., Freeman & Bland-Hawthorn 2002). It is the goal of this work to provide a first step toward the modeling needed to exploit these observations to their fullest potential.

The combination of spatial, kinematic, and chemical data will provide a powerful tool for testing different Galaxy formation models. Historically, metallicity gradients have acted a primary motivator in formulating hypotheses: large-scale metallicity gradients are associated with a rapid, semicontinuous collapse (Eggen et al. 1962, hereafter ELS62); homogeneous metallicity distributions are associated with chaotic assembly from fragments (Searle 1977; Searle & Zinn 1978, hereafter SZ78). While there are no well-motivated models that predict these opposite extremes from first principles, the poles of debate set by ELS62 and SZ78 serve as important straw-man theories for shaping ideas and testing data. Nevertheless, realistic models will always fall into less idealized categories. For example, our ΛCDM-based model relies entirely on a hierarchical origin for the stellar halo, yet predicts some nonnegligible metallicity gradients (see below). Likewise, models that allow significant "rapid" in situ star formation necessarily contain some accreted stellar material as a result of having a background hierarchical cosmology (e.g., Renda et al. 2005). Clearly, only in combination with spatial and kinematic data can chemical abundance data be used to its full potential.

Numerous results over the past decades support the validity of the hierarchical model of structure formation (White & Rees 1978; Blumenthal et al. 1984). In this model, the expectation for stellar halos of galaxies like the Milky Way is that they form in large part by phase mixing of tidal debris from the numerous accreted satellites. Although the dynamical evolution of galaxy halos has been extensively modeled, and we have now predictions for the phase-space distribution of both dark matter and stars in the halo of the Galaxy (e.g., Johnston 1998; Helmi et al. 1999, 2003; Bullock et al. 2001; Abadi et al. 2006; Bullock & Johnston 2005; Diemand et al. 2005; Moore et al. 2006), currently there are no clear predictions for the associated phase-space distribution of chemical elements.

Intuitively, one expects stochastic accretions to leave peculiar signatures in both the kinematics and chemical abundances of present-day stars. Some observational evidence in that respect is indeed found in our Galaxy. The halo contains stars that stand out in both metallicity and velocity (Carney et al. 1996; Nissen & Schuster 1991, 1997; Majewski et al. 1996; Chiba & Beers 2000; Altmann et al. 2005), as does the disk (Helmi et al. 1999, 2006; Navarro et al. 2004). Similar evidence has been found in M31, the only other spiral galaxy whose stellar halo has been studied at a comparable level of detail as that of the Milky Way (Ferguson et al. 2002, 2005; Reitzel & Guhathakurta 2002; Bellazzini et al. 2003; Guhathakurta et al. 2006b). The giant stellar stream in M31, a merger debris extending more than 100 kpc to the southeast of M31's disk, stands out from the background halo not only in stellar overdensities and kinematics (Ibata et al. 2001, 2004; Guhathakurta et al. 2006a), but also in metallicity (Ferguson et al. 2002).

Over the next decade an immense amount of data will become available for stars in the Galaxy from both astrometric and

[1] Van Vleck Observatory, Wesleyan University, Middletown, CT 06459; afont@astro.wesleyan.edu.

[2] Center for Cosmology, Department of Physics and Astronomy, University of California, Irvine, CA 92687.

[3] Harvard-Smithsonian Center for Astrophysics, 60 Garden Street, Cambridge, MA 02138.

TABLE 1
PROPERTIES OF THE SIMULATED STELLAR HALOS

Halo	No. of Accreted Luminous Satellites	No. of Surviving Luminous Satellites	$M_*^{\rm halo}$ (<300 kpc) ($10^9\ M_\odot$)	80% Halo Accretion Time (Gyr)	Time of Last >10% Merger (Gyr)	No. of Particles in Stellar Halos
H1.....	115	18	4.16	5.3	8.3	1908100
H2.....	102	6	3.26	7.0	9.2	1890197
H3.....	106	16	4.17	7.4	8.9	1689035
H4.....	97	8	4.11	6.3	8.3	1628686
H5.....	160	18	2.40	2.1	10.8	2531076
H6.....	169	16	2.45	6.2	10.5	2873983
H7.....	102	20	2.44	4.4	7.4	1797682
H8.....	213	13	2.58	7.1	9.3	4246733
H9.....	182	15	2.52	1.5	10.0	2528762
H10.....	156	13	3.12	2.9	9.7	2785418
H11.....	153	10	2.56	7.2	9.0	2598580

NOTE.—Times refer to look-back times.

spectroscopic surveys, e.g., from the astrometric satellite *Gaia* (e.g., Perryman et al. 2001), the Radial Velocity Experiment (RAVE; e.g., Steinmetz 2003), and the Sloan Extension for Galactic Underpinnings and Exploration (SEGUE).[4] Positions, line-of-sight velocities, and proper motions will be measured for millions of stars in the halo, enabling the full phase space to be reconstructed. Similarly, high-accuracy, wide-field measurements of stellar spectra will allow the mapping of the Galaxy in chemical abundances. These studies will not only constrain cosmology and galaxy formation (e.g., Bullock et al. 2001) but also test ideas about first light and reionization (e.g., Tumlinson et al. 2004). With the upcoming observational data, the goal of putting together the history of our Galaxy is finally becoming feasible. It is therefore important to have theoretical predictions for the combined kinematic and chemical abundance distributions, as well as to have a coherent theoretical framework for interpreting the upcoming results.

Although future surveys promise to provide detailed maps of the chemical and phase-space structure of the Galaxy, we may worry that ours is but one among many galaxies of its size. How typical is our galaxy? How can it be used to constrain general ideas about cosmology and galaxy formation if it is atypical in some way? Fortunately, in the context of ΛCDM, we have well-defined expectations for variations in the formation times and accretion histories of Milky Way–size galaxies, and this idea is at the heart of our exploration. For example, Mouhcine et al. (2005a, 2005b) recently have estimated the metallicities of the inner halos of several nearby spiral galaxies and find that they are quite metal-rich compared to the stellar halo of the Milky Way. They go on to suggest that the Milky Way is not typical for a normal spiral galaxy of its luminosity. As discussed below, if this result holds, then our models provide a straightforward interpretation: that the Milky Way has experienced fewer-than-average metal-rich accretion events, those being either massive (LMC-size) objects or less massive but late-accreted ones. Indeed, phase-space information could test ideas of this kind, specifically by revealing few major accretion events and many more lower mass accretions.

The modeling of the chemical evolution of the Galaxy in a realistic cosmological context is just beginning to be explored (e.g., Bekki & Chiba 2001; Brook et al. 2003, 2004). Recent advances in modeling techniques, like the advent of "hybrid" methods, allow us to address this problem with greater resolution. Hybrid methods enable the modeling of star formation and chemical enrichment with detailed semianalytical prescriptions and at the same time provide the detailed dynamics via the coupled *N*-body simulations (e.g., Kauffmann et al. 1999; Springel et al. 2001). In this study we use a previously developed hybrid method (Bullock & Johnston 2005; Robertson et al. 2005; Font et al. 2006b) to explore the phase-space distribution of chemical abundances in a series of Milky Way–type galaxy halos formed in a ΛCDM universe ($\Omega_m = 0.3$, $\Omega_\Lambda = 0.7$, $h = 0.7$, and $\sigma_8 = 0.9$).

A description of our sample of stellar galaxy models is given in § 2. In § 3 we present results on the spatial distribution of [Fe/H] and [α/Fe] chemical abundances in these stellar halos and propose a criterion for detecting cold stellar streams based on their [α/Fe] abundances. In § 4 we discuss our results and compare them with the available observations, and in § 5 we conclude.

2. THE SAMPLE OF MILKY WAY–TYPE STELLAR HALOS

In a previous study Bullock & Johnston (2005) have presented a sample of 11 stellar halos of Milky Way–type galaxies assembled hierarchically from accreted satellite galaxies in a ΛCDM cosmology. The physical properties of the simulated halos are summarized in Table 1. The merger histories of these halos have been specifically selected not to have high-mass recent mergers, so as to maximize the probability that it will host a disk galaxy like the Milky Way (e.g., Wyse 2001). Our model stellar halos have mass, density profile, and total luminosity similar to the Galactic halo. The models also obtain roughly the same number of surviving satellite galaxies as in the Milky Way and match their physical properties: the stellar mass–circular velocity relation, M_*-$v_{\rm circ}$, for Local Group dwarfs; and the distribution of surviving satellites in luminosity, central surface brightness, and central velocity dispersion.

In this paper we extend our models to include chemical evolution with the prescriptions of Robertson et al. (2005). These include enrichment from both Type II and Type Ia supernovae and feedback provided by supernovae blow out and winds from intermediate-mass stars. We follow the chemical evolution of each satellite galaxy accreted onto the main Galaxy and trace the buildup of a series of metals, such as Fe or α-elements. Each star particle in the simulations has assigned a set of [Fe/H] and [α/Fe] abundance[5] ratios determined by the star formation history of the satellite in which the star originated. The coupled

[4] See http://www.sdss.org.

[5] The [α/Fe] ratio is defined as the average of [Mg/Fe] and [O/Fe] ratios and used hereafter in the paper.

N-body simulations resolve each Milky Way–type stellar halo with a few million particles and allow us to explore the phase-space distribution of chemical abundances in unprecedented detail.

3. RESULTS

3.1. *Global Properties of the Simulated Halos*

Tidal streams in the halo display various degrees of spatial coherence, given their different times of accretion and orbital properties. Similarly, we expect to see various degrees of coherence in the chemical abundance space, given the different star formation and chemical enrichment histories of their progenitor satellites.

Figure 1 shows the present-day ($t = 0$) spatial distribution of [Fe/H] and [α/Fe] abundance ratios for halos H1–H8. The maps span 300 kpc on a side (x- and z-directions, respectively) and 300 kpc in depth (y). Each pixel represents a color-coded chemical abundance, calculated as the average [Fe/H] or [α/Fe] of all stars included in a volume $0.25 \times 300 \times 0.25$ kpc^3. Our models show that inner regions of the halos ($r < 50$ kpc) are consistently more homogeneous than the outer ones, both in terms of the spatial distribution of stars and in the overall chemical abundances. This is because the inner halo builds up rapidly, with most of its stellar mass already in place in the first 4–5 Gyr of Galaxy evolution (Bullock & Johnston 2005; Font et al. 2006b), and at these times the dynamical timescales were shorter and phase mixing more efficient. The spatial distribution of the stars has been discussed in more detail by Bullock & Johnston (2005), who also note a similar behavior in the surface brightness and velocity distribution of halo stars. Here we concentrate on the corresponding [Fe/H] and [α/Fe] distributions.

We find that the inner $\sim$50 kpc regions are, on average, metal enriched ([Fe/H] ≥ -1.2), and we trace this to the metal contribution of a few massive ($M_* \sim 10^9\ M_\odot$) satellites accreted early on, which contribute a significant fraction (40%–60%) to the total stellar mass of the halo (Font et al. 2006b). The rapid growth of these satellites at early times fueled an intense star formation, and therefore, at the time of accretion the satellites were already enriched in [Fe/H]. In the outer regions ($r > 50$ kpc) the streams are more spatially separated, and their various chemical enrichments are more distinct. Both metal-poor and metal-rich streams are present, with the more metal-poor ones originating in satellites with low star formation rates (these are typically low-mass satellites). A more detailed discussion of radial distributions of stars is given in § 3.3.

Figure 2 shows the average [Fe/H] and [α/Fe] for all our Milky Way–type halos. The general trend in our simulations is that the more massive a stellar halo, the more chemically evolved it is, i.e., the higher [Fe/H] and lower [α/Fe] it has [these relations are independent of the cutoff radius assumed for $M_*(r)$]. The [Fe/H]-M_* trend in Figure 2 is consistent with having the same slope as that of the well-known relation between metallicity and luminosity seen in low-mass galaxies, [Fe/H] $\propto M_*^{-2/5}$ (*dashed line*). We note that our chemical feedback model is normalized such that surviving satellites at $z = 0$ match the observed metallicity-luminosity relation for Local Group galaxies (Larson 1974; Dekel & Silk 1986; Dekel & Woo 2003). It is interesting, however, that a similar relation propagates to the stellar halos themselves. This follows from the fact that the slope of the relation for satellite galaxies is governed by their parent halo potential well depths. Therefore, disrupted satellites also follow a [Fe/H] $\propto M_*^{-2/5}$ relation (see Fig. 4 in Font et al. 2006b), but with a lower [Fe/H] normalization, because these systems tend to be accreted earlier and are less evolved (Font et al. 2006b; Robertson et al. 2005). The same relation propagates to a *stellar halo* mass-metallicity relation, because stellar halo mass correlates strongly with the number of disrupted *massive* satellites (see § 3.2). The more massive disruptions a stellar halo contains, the more metal-rich the stellar halo becomes. Similarly, because its progenitors are massive, they are more metal-rich, and the halo is higher metallicity as a result.

Our results suggest that the hierarchical assembly is an important factor in determining the metallicity-mass relation for stellar halos. A similar argument can be extended to qualitatively understand the observed trend presented by Mouhcine et al. (2005b), who show that low-luminosity spiral galaxies have more metal-poor central stellar halos than do high-luminosity spirals. This qualitative trend can be explained in a hierarchical scenario; low-luminosity spirals tend to have accretion histories dominated by correspondingly lower luminosity dwarfs. Lower luminosity dwarfs are more metal-poor and thus produce lower metallicity stellar halos. While one can derive the [Fe/H]-M_* relation based on simple scaling arguments that relate the metal loss to the depth of the central galaxy's dark matter halo (e.g., Larson 1974; Tinsley 1980), this does not necessarily imply that the relation forms in situ.

We caution that for a complete understanding of the origin of the relation (both of its shape and normalization), one needs a more accurate treatment of gas physics processes in satellites after they are accreted onto the main halo. These effects are not currently included in our models, but we expect them to be of second order to the hierarchical mass assembly.

3.2. *Mass Accretion Histories and Halo Metallicities*

We can verify the hierarchical origin of the [Fe/H]-M_* relation by investigating the mass accretion histories of the stellar halos. Given that in a typical mass accretion history the few massive satellites contribute significantly to the final stellar mass, we expect the overall halo metallicity (and hence the [Fe/H]-M_* trend) to be determined mainly by these massive accretions. The time of accretion of massive satellites is also a related factor; satellites accreted later are likely to be more metal-rich.

Figure 3 plots for each stellar halo in our sample the look-back time of accretion of the most massive progenitors, specifically an average over those satellites that contribute more than 10% to the total stellar fraction. The general tendency is that more massive halos assemble more recently. In addition, for halos of the same mass, the spread in [Fe/H] can be also explained by differences in their formation time (e.g., the three halo models with $M_* \sim 1.5 \times 10^9\ M_\odot$). Therefore, a protracted assembly of the higher mass stellar halos seems to be at the origin of the [Fe/H]-M_* relation (see also similar results of Renda et al. 2005).

3.2.1. *A Test Case: Milky Way and M31*

We further illustrate the relation between mass accretion histories and the overall metallicities with the case of Milky Way and M31. These are two large galaxies with roughly the same luminosity, but the Milky Way halo is more metal-poor than that of M31, perhaps by as much as 1 dex. The metallicity distribution function (MDF) in the Milky Way halo peaks around [Fe/H] $= -1.5$ (Laird et al. 1988; Carney et al. 1996), whereas the MDFs measured at several locations in the *inner* "halo" of M31 peak at values between [Fe/H] $\simeq -0.4$ and -0.7 (Reitzel & Guhathakurta 2002; Bellazzini et al. 2003). Although, as discussed below, the outer halo of M31 at [Fe/H] ~ -1.2 may be a more realistic estimate of the true underlying stellar halo component of this galaxy (Guhathakurta et al. 2006b).

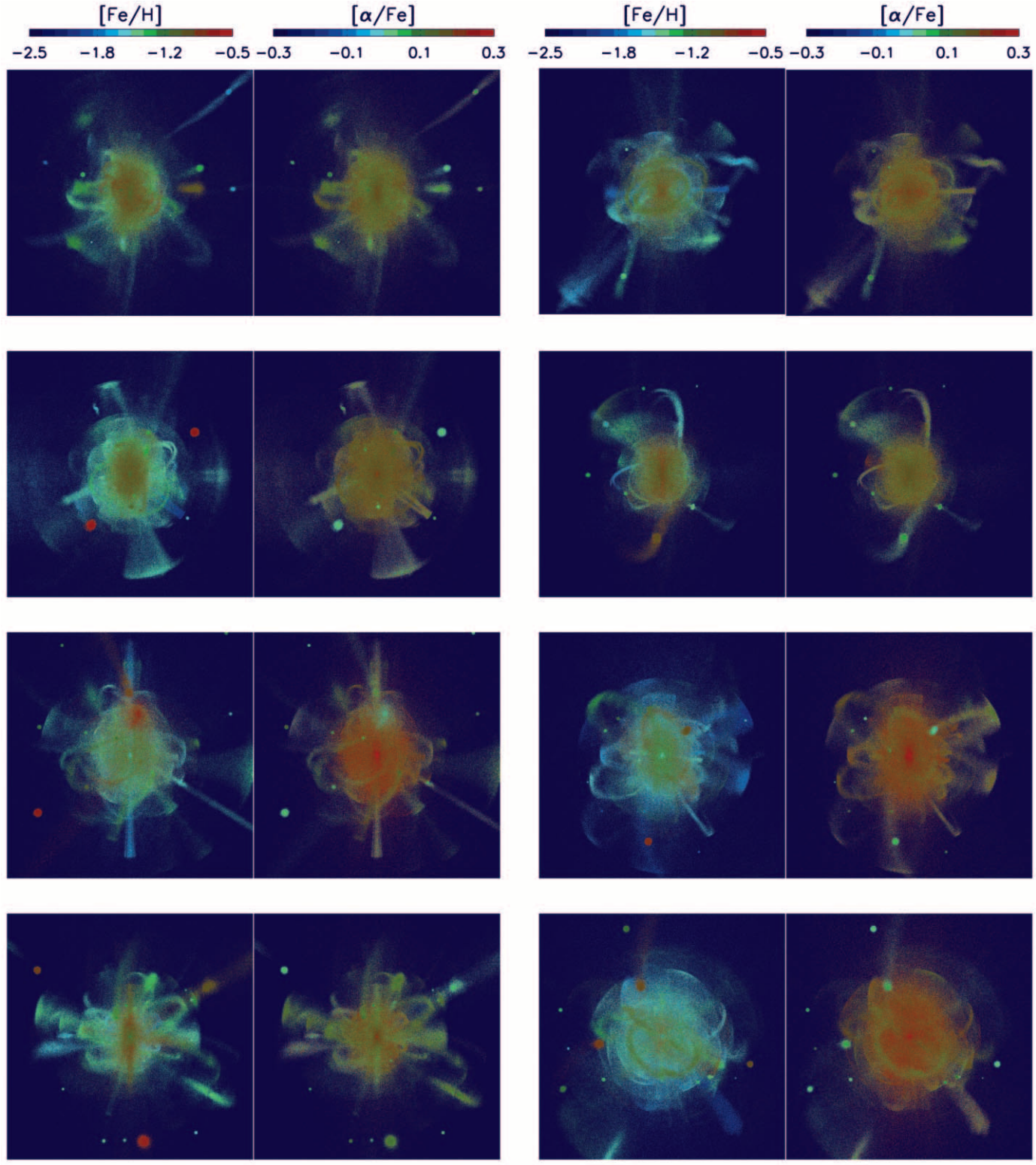

FIG. 1.—The (x, z) projections of chemical abundances in halos H1–H8 (*top left to bottom right*). For each halo we show side by side the star particles color-coded in [Fe/H] (*left subpanels*) and in [α/Fe] (*right subpanels*). The maps span 300 kpc on a side. Each pixel in these maps extends 0.25 kpc in the x- and z-directions and 300 kpc in the y-direction (i.e., in depth). The [Fe/H] and [α/Fe] values are mass-weighted averages over all stars contained in each pixel.

Figure 4 shows the mass accretion patterns, expressed as the fractional contribution of accreted satellites to the total stellar mass of the inner halo, for two halo models similar to the inner Milky Way and M31: halo H5, with $\langle[\mathrm{Fe/H}]\rangle \simeq -1.3$, and halo H4, with $\langle[\mathrm{Fe/H}]\rangle \simeq -0.9$ (these are also the most extreme cases in our sample). The more metal-poor halo has one major accretion of stellar mass, $M_* \sim 10^8$–$10^9\ M_\odot$, accreted about 11 Gyr ago, while the more metal-rich halo has two major accretions, both of masses $M_* \simeq 10^9\ M_\odot$ and accreted about 8.5 Gyr ago. Thus, the most massive, metal-rich halo had an assembly history

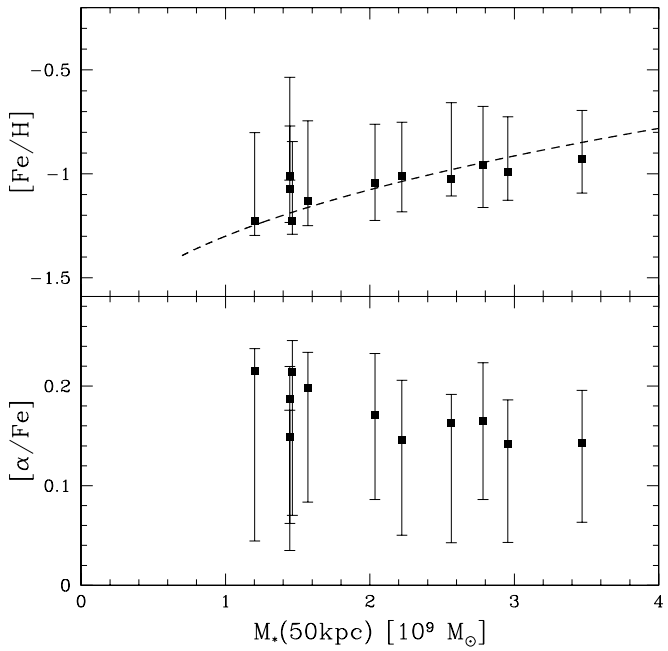

FIG. 2.—Mass-weighted [Fe/H] and [α/Fe] average values vs. stellar mass for halos H1–H11. Averages are calculated within $r < 50$ kpc, a cutoff value that approximates the inner few tens of kiloparsecs currently probed by observations. The dashed line in the top panel corresponds to the $[\mathrm{Fe/H}] \sim M_*^{2/5}$ fit of Dekel & Woo (2003). Error bars represent weight-averaged 25% and 75% values of the absolute spread in abundance ratios.

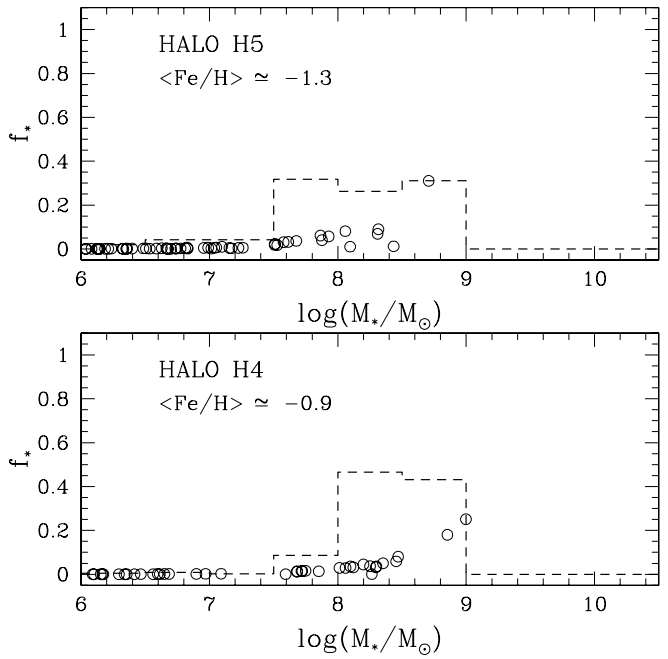

FIG. 4.—Mass accretion histories expressed as the stellar fraction f_* of the inner ($r < 50$ kpc) halo vs. the stellar mass M_* of the contributing satellites. The top panel corresponds to halo H5, a metal-poor halo with $\langle[\mathrm{Fe/H}]\rangle \simeq -1.3$, and the bottom panel corresponds to halo H4, a metal-rich halo with $\langle[\mathrm{Fe/H}]\rangle \simeq -0.9$. Circles show individual contributions of satellites to the stellar fraction, and dashed lines show their cumulative contribution.

that includes more massive progenitors that were accreted later. The inference from these results is that the difference in metallicities between the two galaxies can be explained if M31 experienced one or two more massive accretions than the Milky Way and/or a protracted merger history.

However, we note that the metallicity measurements in both Milky Way and M31 are not yet completely reliable. One reason is that most observations probe only the inner few tens of kiloparsecs and therefore may not be representative of the entire halos or may include additional galactic components. For example, recent observations in M31 extending further out into the halo find $[\mathrm{Fe/H}] \simeq -1.2$ for stars beyond 60 kpc, suggesting that the high metallicities measured in the inner regions include the contribution from M31's extended bulge (Guhathakurta et al. 2006b; Kalirai et al. 2006, Gilbert et al. 2006). Additional contamination may come from the recently discovered disklike component extending out to ~70 kpc (Ibata et al. 2005; Irwin et al. 2005). There are also differences in the measurement methods. In the Milky Way metallicities are determined spectroscopically, while in M31 they are mostly determined photometrically (but see new spectroscopic measurements of Ibata et al. [2004] and Guhathakurta et al. [2006a]). It is therefore unclear whether the metallicity discrepancies between the two galaxies are real, but ongoing wide-field spectral studies in these galaxies may be soon able to answer this problem. Nevertheless, our results are more general and suggest ways in which massive accretion events can increase the average metallicities of halos (e.g., one massive dwarf galaxy, $M_* \simeq 10^9\ M_\odot$, accretion is sufficient to increase the average metallicity of a Milky Way–type halo by about 0.5 dex).

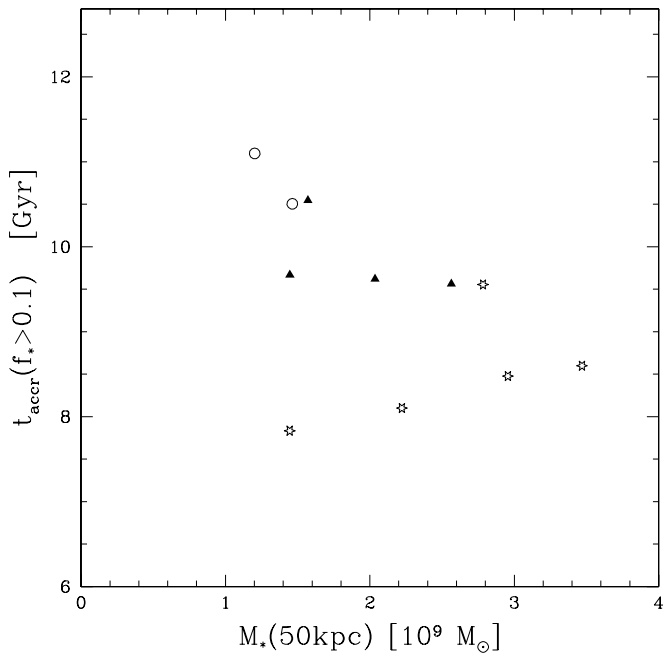

FIG. 3.—Look-back time of accretion of the most massive satellites (calculated as the average t_{accr} of those satellites that contribute $\geq$10% to the total mass of the stellar halo) vs. stellar mass of the inner halo, M_*(50 kpc). Stars correspond to the most metal-rich halos, triangles correspond to halos of intermediate [Fe/H], and circles correspond to those of lowest [Fe/H] in our sample.

3.3. *Radial Distributions*

As explained in § 1, metallicity gradients are a powerful tool for constraining the timescale of formation of galaxies. An often-cited hypothesis is that hierarchical formation will result in a negligible metallicity gradient. In detail, however, some variations may occur, particularly in regions that continue to assemble until recent times.

The radial distributions of [Fe/H] and [α/Fe] abundances for all simulated halos are shown Figures 5 and 6. Indeed, the distributions show a systematic lack of large-scale gradients, yet many show variations over scales of a few tens of kiloparsecs.

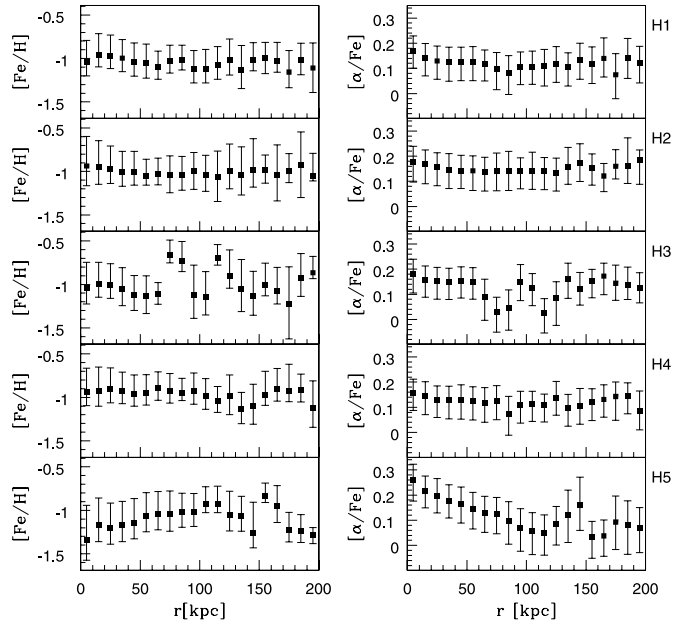

FIG. 5.—Radial distributions of [Fe/H] (*left*) and [α/Fe] (*right*) for halos H1–H5 (*top to bottom*). The chemical abundances are weighted averages in radial shells of width $dr = 10$ kpc. Error bars represent weight-averaged 25% and 75% values of the absolute spread in abundance ratios within each radial bin.

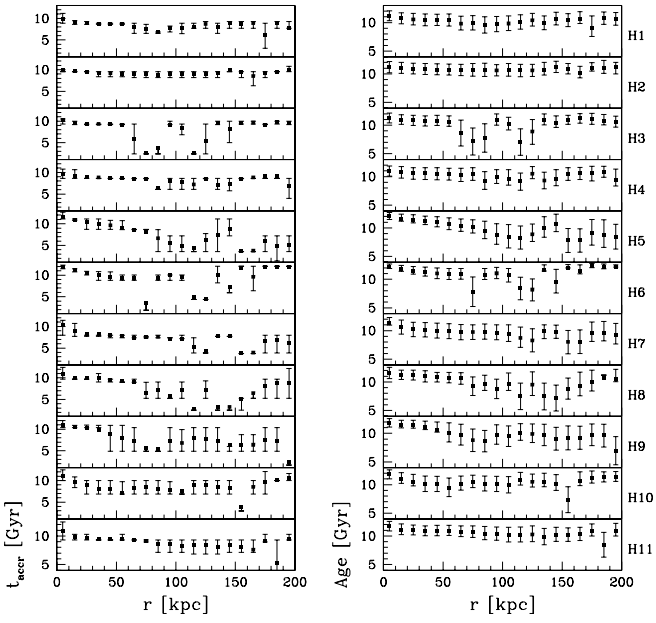

FIG. 7.—Radial distributions of look-back accretion times (*left*) and ages of stellar populations (*right*) for halos H1–H11 (*top to bottom*). The abundance ratios are weighted averages within radial bins of 10 kpc. Error bars represent weight-averaged 25% and 75% values of the absolute spread in abundance ratios in each radial bin.

The lack of large-scale gradients can be explained by examining the mass accretion patterns of our simulated halos. The bulk of the stellar halos form early, both in the inner and outer regions. The outer halos continue to accumulate stellar debris up to more recent times ($\sim$5–6 Gyr ago), but this represents only a small fraction of the total stellar mass (Bullock & Johnston 2005; Font et al. 2006b). Therefore, even if the later assembly of the outer halo favors an influx of chemically enriched material, this is not sufficient to create significant large-scale gradients. Moreover, the chemical abundances are directly correlated with the ages of the stars, rather than with the time of accretion. Figure 7 plots the distribution of look-back accretion times (*left*) and the ages of stellar populations (*right*) versus the radial distance for all halo models. As this figure shows, even if the stellar material is accreted recently, it usually contains a mixture of both young and old stars that dilutes the metallicity differences.

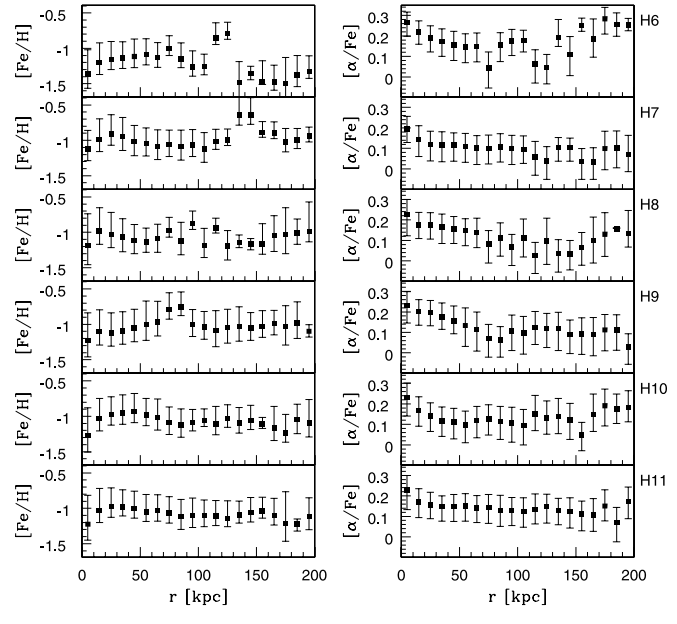

FIG. 6.—Same as Fig. 5, but for halos H6–H11 (*top to bottom*).

Many of our halos do show distinct small-scale abundance gradients. For example, in halos H5, H6, and H9 the average [Fe/H] increases with r in the inner 100 kpc (similarly, [α/Fe] decreases over the same distance). The gradients in these halos arise from the spatial distribution of their stellar populations. Figure 7 shows that the inner regions of these three halos contain mostly old ($\sim$10 Gyr) stellar populations, whereas the outer regions have on average stellar populations a few Gyr younger. Perhaps the only systematic small-scale trend in our simulations is the low [Fe/H] in the inner 10 kpc (see the innermost radial bin in Fig. 6). These results have implications for searches for the "first" stars in the stellar halo and complimentary attempts to use the metallicity distribution function to constrain the nature of reionization and Population III star formation (e.g., Tumlinson et al. 2004; Beers et al. 2005). Specifically, we find that the lowest metallicity stars, as well as the earliest formed stars, are expected to inhabit the most central regions of the Galaxy. For example, our simulations suggest that about 30%–50% of either the 1% lowest [Fe/H] stars or the 1% oldest stars lie within the inner 10 kpc of the Galaxy.[6] Thus, general attempts to use observed metallicity distribution functions to constrain early chemical enrichment must take special care to account for spatial biases in observational samples of stars.

The radial distributions of accretion times, ages, and chemical abundances give an insight into the composition of stellar populations in the simulated halos. Our results suggest that stellar halos of galaxies like the Milky Way should contain a large fraction of old (>10 Gyr) stellar populations that were accreted in the first few Gyr of the mass assembly. In addition to the underlying

[6] The radial distribution of the 1% oldest stars is in general agreement with that reported by White & Springel (2000); however, our results regarding the distribution of the lowest metallicity stars disagree. White & Springel (2000) find that about 60% of the 1% oldest stars are located within the inner 10 kpc, whereas only 16% of the 1% lowest metallicity stars are within the same radius.

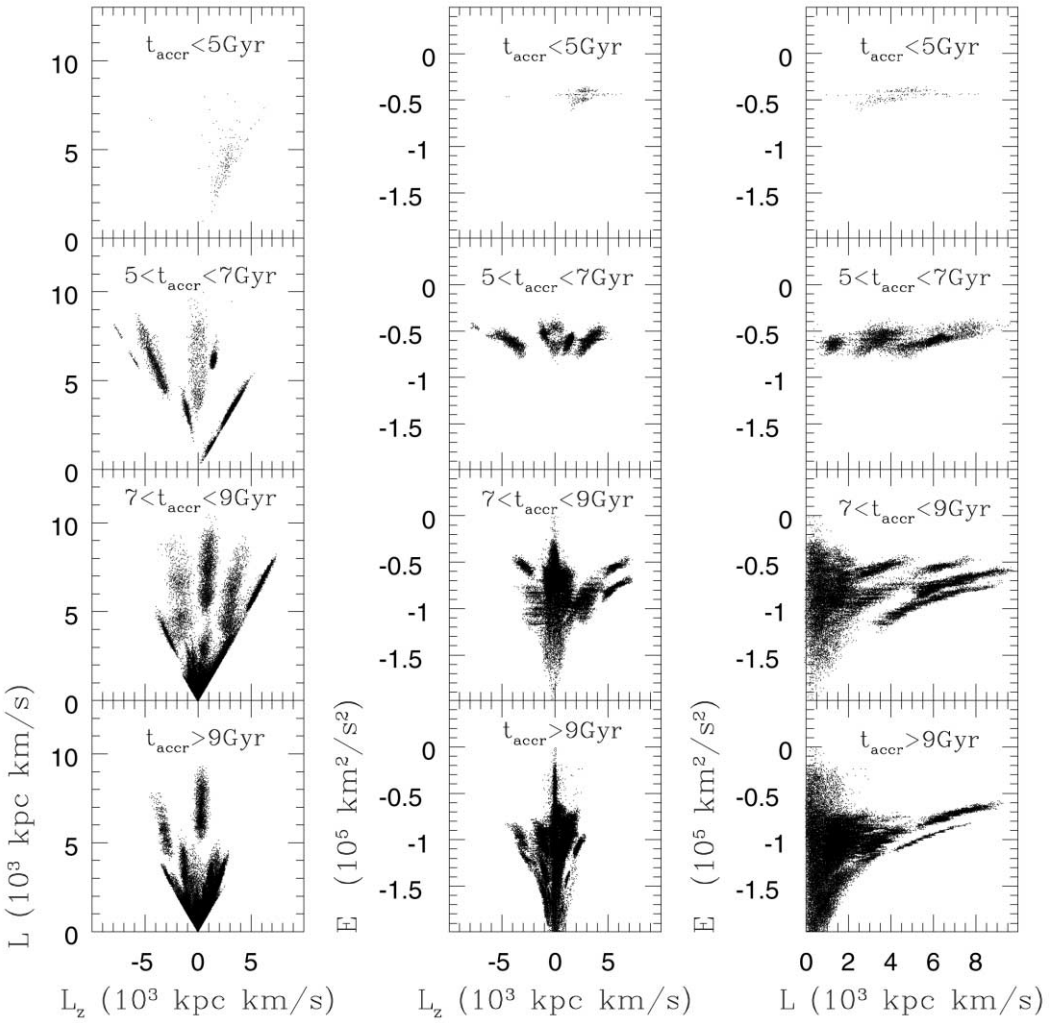

FIG. 8.—Distribution of stars in halo H1 in L_z-L space (*left*), in E-L_z (*middle*), and in E-L (*right*). Different panels correspond to different look-back accretion times of the satellites where stars originate from.

population of old stars, some halos contain small fractions of intermediate-age (∼7–10 Gyr) populations. Irrespective of their age, stars can be either metal-poor or metal-rich, depending of the mass and star formation rate of their progenitor satellite.

Interestingly, in terms of its age and metallicity distributions, the Milky Way halo lies at the edge of our sample-simulated halos. The stars in the Milky Way halo are mostly old and metal-poor, whereas in our models a significant number of old stars are already metal enriched. (Note, however, that the typical observations cover only the inner ∼10–20 kpc of the halo, and in this range some of our halos are old and metal-poor.) Our results seem to suggest that the Milky Way halo is an atypical case in the range of galaxies of similar mass. The metallicity constraints rule out an accretion of a massive ($M_* \sim 10^9\ M_\odot$) halo progenitor at early times when the bulk of the halo formed. We also note that recent observations show that many other bright spiral galaxies of similar mass have more metal-rich halos than that of the Milky Way. A more detailed discussion of these observations is given in § 4.1.

3.4. *Mining the Halo for Stellar Streams*

Tidal streams are fossil records of past accretions and therefore can be used to reconstruct the merger histories of galaxies. Their detection, however, is difficult due to their low surface brightness and the loss in spatial coherence the longer they orbit in the Galaxy. The identification of stellar streams can be improved by extending the parametric space to include new dimensions like the kinematic parameters and chemical abundances.

If kinematic data are available from observations, one can use the (E, L_z, L) space to identify stellar streams. This parametric space is particularly useful for epochs of slow evolution, when the time required for stars to exchange energy and angular momentum is long compared with the age of the Galaxy, and E, L_z, and L can be approximated as invariants of motion (e.g., Eggen et al. 1962). In this case, the tidal debris from different accretions is expected to clump in distinct locations in this space. Numerical simulations of satellite accretions in a fixed potential (Helmi & de Zeeuw 2000) and later extended to include a time-evolving gravitational potential (Knebe et al. 2005) confirm that this is indeed the case.

Our modeling also includes a time-evolving gravitational potential that grows with the mass of the Galaxy (see Bullock & Johnston 2005 for details). In agreement with Knebe et al. (2005), we find that the tidal debris can still be recovered in the (E, L_z, L) space. Figure 8 plots the distribution of halo H1 stars in

the L_z-L, E-L_z, and E-L planes at different ranges of look-back accretion times of the progenitor satellites. This shows that the recent accretions ($t_{\rm accr} \leq 7$–9 Gyr) occupy relatively distinct locations in these planes and their identification is therefore possible.

The clumps in the low-E and low-L regime are more difficult to separate, in part because of their superposition, but also because this is also the regime of rapid growth of the Galaxy when the energy and angular momentum of stars change significantly. Additional effects like the interaction between satellites and the nonaxisymmetric oscillations in the Milky Way potential, not modeled in our study, will further disperse the stars in phase space (Mayer et al. 2002).

The kinematic identification of stellar streams in the halo requires high-accuracy measurements of proper motions over extensive areas of the sky. Future astrometric Galactic surveys such as *Gaia* will be able to provide these data and identify some of these clumps (Helmi & de Zeeuw 2000).

Chemical abundances can be used as an additional dimension to the (E, L_z, L) parametric space to investigate the origin of stars (e.g., Bekki & Chiba 2001; Dinescu 2002). By separating the available kinematic parameters in different metallicity ranges, some observational studies have found stars that stand out from the rest of the halo, implying a merger origin (e.g., Carney et al. 1996; Majewski et al. 1996). However, given that even stars from the smooth halo may originate in mergers, it is instructive to investigate whether chemical abundances can provide any new information about the merger history of the Galaxy.

In particular, chemical abundances may be able to constrain the merger time line of the Galaxy. In Figure 8 we have used the time of accretion to separate the clumps in the (E, L_z, L) space. This parameter is not easily measurable, but fortunately, we can use the natural clock provided by the evolution of Fe and α-elements. Each satellite galaxy is expected to have a distinct [α/Fe]-[Fe/H] evolution; however, it has some generic features such as a plateau at high [α/Fe] and low [Fe/H] and then a steady decrease toward high [Fe/H] (both the length of the plateau and the slope of the decrease being modulated by the star formation rate, hence the mass of the satellite). The plateau is maintained by the enrichment in α-elements in Type II supernovae operating on short timescales (of a few Myr), and the [α/Fe] decrease is driven by the later enrichment in Fe produced in Type Ia supernovae. Prolonged episodes of star formation will tend to decrease the [α/Fe] ratios of stars in a satellite. This suggests an association between the time of accretion of satellites and their overall [α/Fe].

Figure 9 plots the weight-averaged [α/Fe] versus [Fe/H] values for satellites accreted onto halo H1, highlighting the times of accretion. This shows that the lowest [α/Fe] values are associated with recently accreted satellites, these systems having more time available to form stellar populations with [α/Fe] below solar. This is more clearly seen in Figure 10, where we plot the distribution of stars in the E-L_z and E-L planes, separated in different [α/Fe] ranges. Most of the stars with [α/Fe] < 0.05 are in the high-energy and high angular momentum regime, associated with recent accretions.

This also suggests that by selecting an [α/Fe] < 0.05 cut, one can effectively remove the bulk of the old, well-mixed halo and identify only the recently accreted streams. Figure 11 illustrates this with a comparison between the surface brightness maps of some of the simulated halos, first by including all stars (*left subpanels*) and alongside including only those stars with [α/Fe] $<$ 0.05 (*right subpanels*). With this cut, the central regions are effectively devoid of the well-mixed streams and contain only the cold streams.

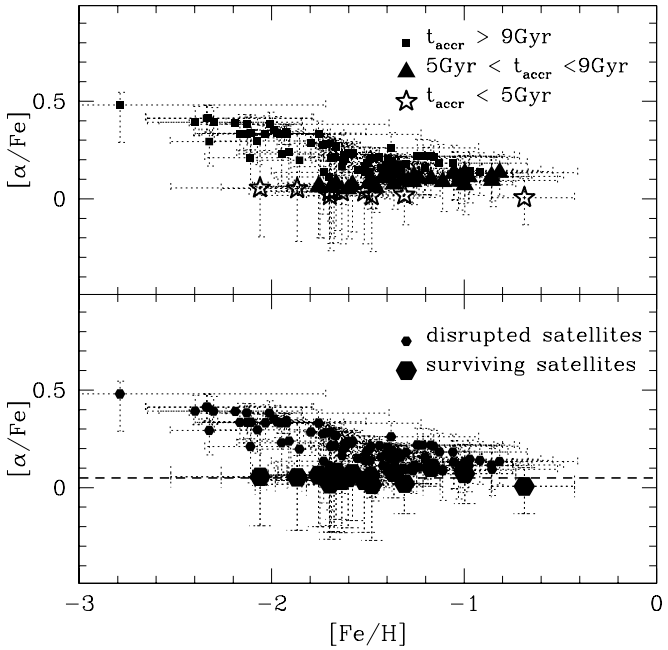

FIG. 9.—The [α/Fe] vs. [Fe/H] for all baryonic satellites accreted onto halo H1. *Top:* Satellites are plotted with different symbols based on their look-back time of accretion; squares denote satellites accreted at $t_{\rm accr} > 9$ Gyr, triangles denote those accreted at $5 < t_{\rm accr} < 9$ Gyr, and star symbols denote those accreted at $t_{\rm accr} < 5$ Gyr. *Bottom:* Small and large symbols denote whether satellites are fully disrupted or still contain some bound material at the present time ($t = 0$), respectively. Error bars in both represent 10% and 90% of the weight-averaged values.

How feasible is our selection method for detecting streams in the halo? Figure 11 shows that even without the [α/Fe] cut the tidal streams are faint. Only a few of these streams, typically one or two per galaxy, can be detected with current capabilities, which have a limiting surface brightness in V-band of $\mu_V \simeq$ 30–31 mag arcsec^{-2}. The proposed method can be used to highlight a few cold streams of about this limiting magnitude in the inner halo.

The prospects for detecting giant stars are also reasonable. Assuming the luminosity of halo stars is similar to that of globular cluster M12 (Hargis et al. 2004), a $10^9\,L_\odot$ halo will contain a few times 10^6 giants (out of these, 10^5 giants will be 1 V-band mag above the horizontal branch [HB], or about 10^4 giants 2 V-band mag above the HB, respectively). According to our models, 1%–10% of the stars meet the [α/Fe] < 0.05 cut. This implies, for example, that a halo survey of 10^5 giants with 1 mag above the HB will contain $\sim 10^3$–10^4 giants in cold streams.

4. COMPARISONS WITH OTHER STUDIES

4.1. *Stellar Halo Metallicities*

A series of recent observational studies have found evidence in support of the idea that the metallicity/age of the Milky Way stellar halo is peculiar. It seems that most other bright spiral galaxies are more metal-rich than the Milky Way (e.g., Mouhcine et al. 2005a). M31 is a prime example, but recent observations show that this is also the case for several spiral galaxies outside the Local Group (Mouhcine et al. 2005b), as it is for about 1000 spiral galaxies in the SDSS sample, as inferred from the average of their colors (Zibetti et al. 2004). Similarly, in terms of their stellar composition, the observations suggest that all halos have an underlying, uniform population of old metal-poor stars and that most luminous galaxies have additional metal-rich populations, which can be either old or intermediate age (e.g., Harris

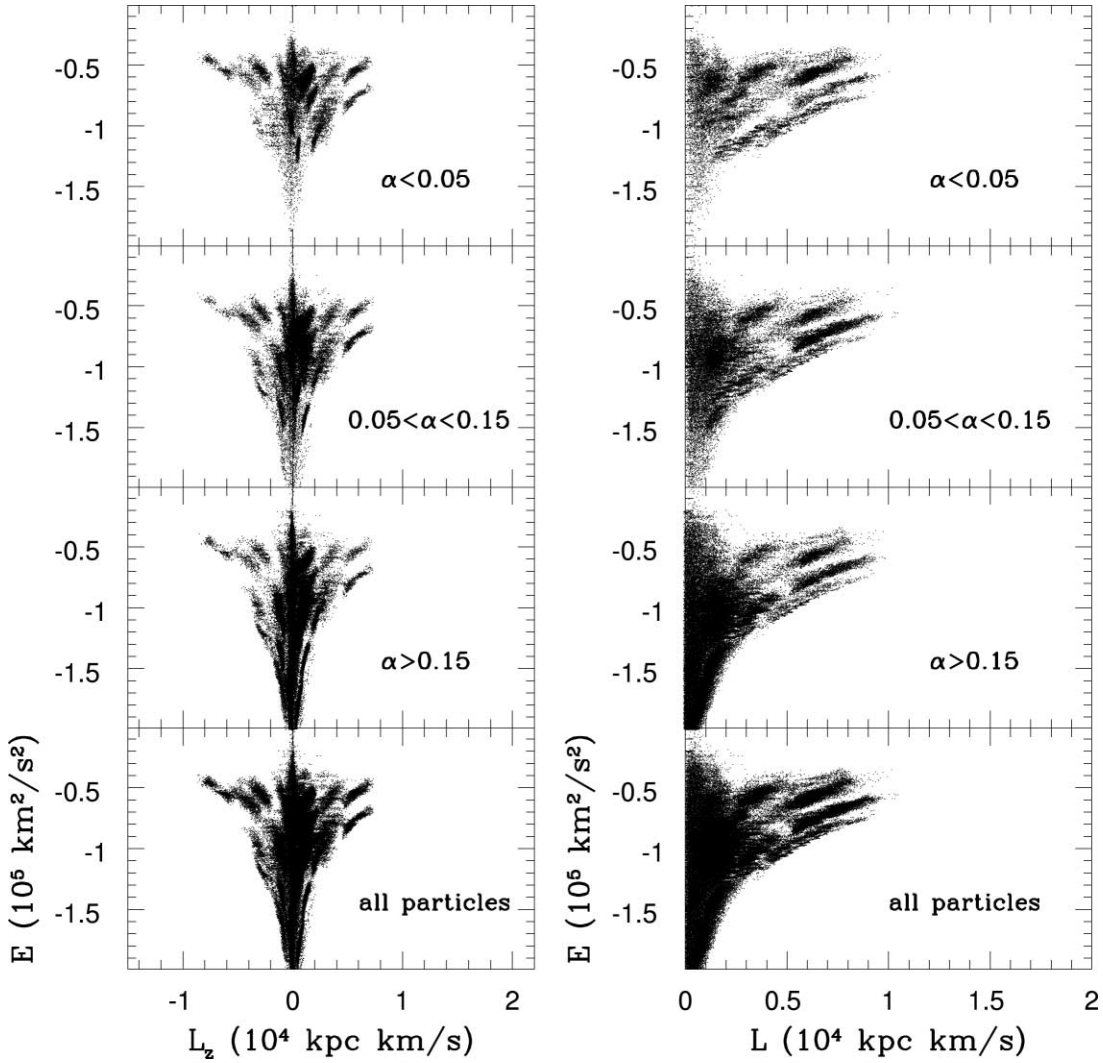

FIG. 10.— Distribution of stars in halo H1 in E-L_z (*left*) and in E-L (*right*). The bottom row shows all stars, while the remaining three rows correspond to different $[\alpha/\mathrm{Fe}]$ ranges.

et al. 1999; Harris & Harris 2002; Bellazzini et al. 2003; Mouhcine et al. 2005b; Gallazzi et al. 2005). As a bright galaxy but with an old and metal-poor stellar halo, the Milky Way may indeed be somewhat rare. Indeed, none of our 11 simulated stellar halos have metallicities as low as that of the Milky Way $\langle[\mathrm{Fe/H}]\rangle_{\mathrm{MW}} \simeq -1.5$, although our most metal-poor halo is close $\langle[\mathrm{Fe/H}]\rangle \simeq -1.3$ (see Fig. 2). Our interpretation would be that the Milky Way is unusually lacking in massive satellite mergers at early times. While rare, this would not be unthinkable within the expectations of ΛCDM, since the average number of accreted massive satellites is small (Zentner & Bullock 2003).

As shown in Figure 2, the metallicities of our simulated halos have a spread of less than 1 dex. This disagrees somewhat with the results of Renda et al. (2005), who report that their simulated halos have a larger [Fe/H] spread, about 1.5 dex, when restricted to have Milky Way–type luminosities. More specifically, the Renda et al. (2005) simulations produce Milky Way–type halos as metal-poor as $\langle[\mathrm{Fe/H}]\rangle \simeq -2$. We suspect that the difference arises from the fact that Renda et al. (2005) allow stellar halo stars to originate via in situ star formation in their simulations, while our stellar halos form entirely from accreted dwarfs. Thus, the metallicity spread in observed halos may provide an interesting avenue for testing the idea of accreted versus in situ stellar halo formation. The small spread in stellar halo metallicities seen by Mouhcine et al. (2005b) may favor an accretion-dominated model, although the evidence is weak as of now. A second difference may arise from the cosmological conditions in Renda et al. (2005), which are set via a semicosmological top-hat sphere with standard CDM fluctuations, while ours rely on extended Press-Schechter within a ΛCDM framework. It is interesting to note that our restriction on accretion histories to be those without recent major mergers would (if anything) bias our distributions to more metal-poor halos, just the opposite bias that would be required to match reconcile our results with those of Renda et al. (2005).

4.2. *Spatial Distributions*

Our models predict that tidal streams from massive satellites should stand out in stellar overdensities and be more metal-rich. The available observational evidence seems to support our finding. A wide survey of the inner M31 halo reveals an increase in metallicity in fields associated with the giant stellar stream (Ferguson et al. 2002). Numerical modeling of the stream finds that the progenitor satellite was indeed massive, $M_* \sim 10^9\ M_\odot$ (Font et al. 2006a; Fardal et al. 2006). Inhomogeneities in color-magnitude diagrams are also seen in the M31 halo and are believed to be

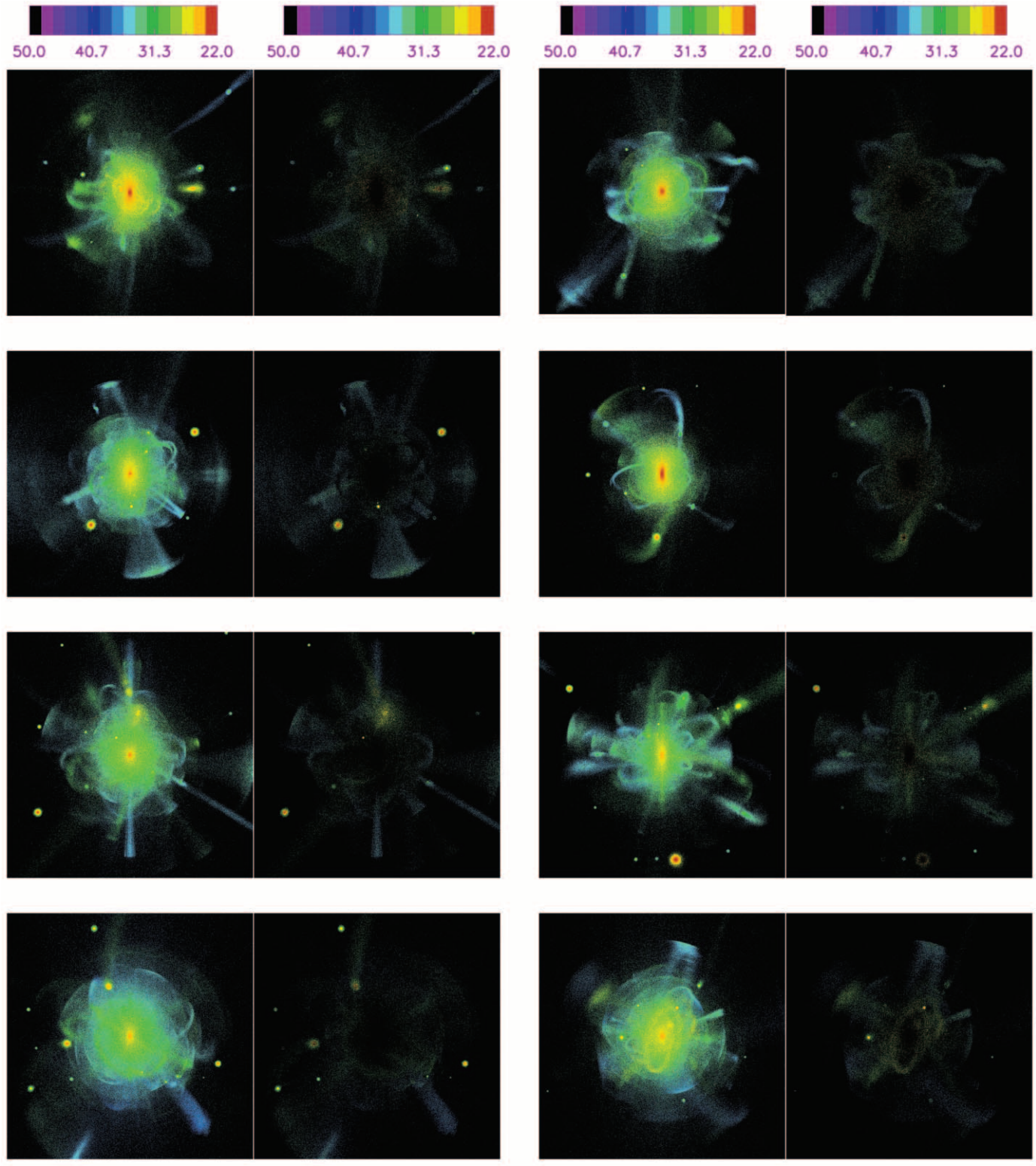

FIG. 11.—The *V*-band surface brightness maps for halos H1, H_2, H3, H4, H5, H7, H8, and H10 (*top left to bottom right*). Left subpanels show the surface brightness map of all stars, and right subpanels show the corresponding surface brightness of stars with $[\alpha/\mathrm{Fe}] < 0.05$. All maps span 300 kpc on a side.

associated with satellite accretions (Brown et al. 2003; Ferguson et al. 2005).

While metallicity inhomogeneities are commonly detected, the observational evidence regarding radial gradients is so far inconclusive. Studies of globular clusters (e.g., Searle & Zinn 1978; Zinn 1993) or of the low-metallicity stars in the Galaxy (Beers et al. 2005) do not show obvious gradients in [Fe/H]. However, some studies report a decline of $[\alpha/\mathrm{Fe}]$ ratios of halo stars with radial distance in the Galaxy (Nissen & Schuster 1997). In M31, measurements in several fields extending up to 40 kpc in the halo are consistent with a small, less than 1 dex, [Fe/H] radial gradient (Bellazzini et al. 2003).

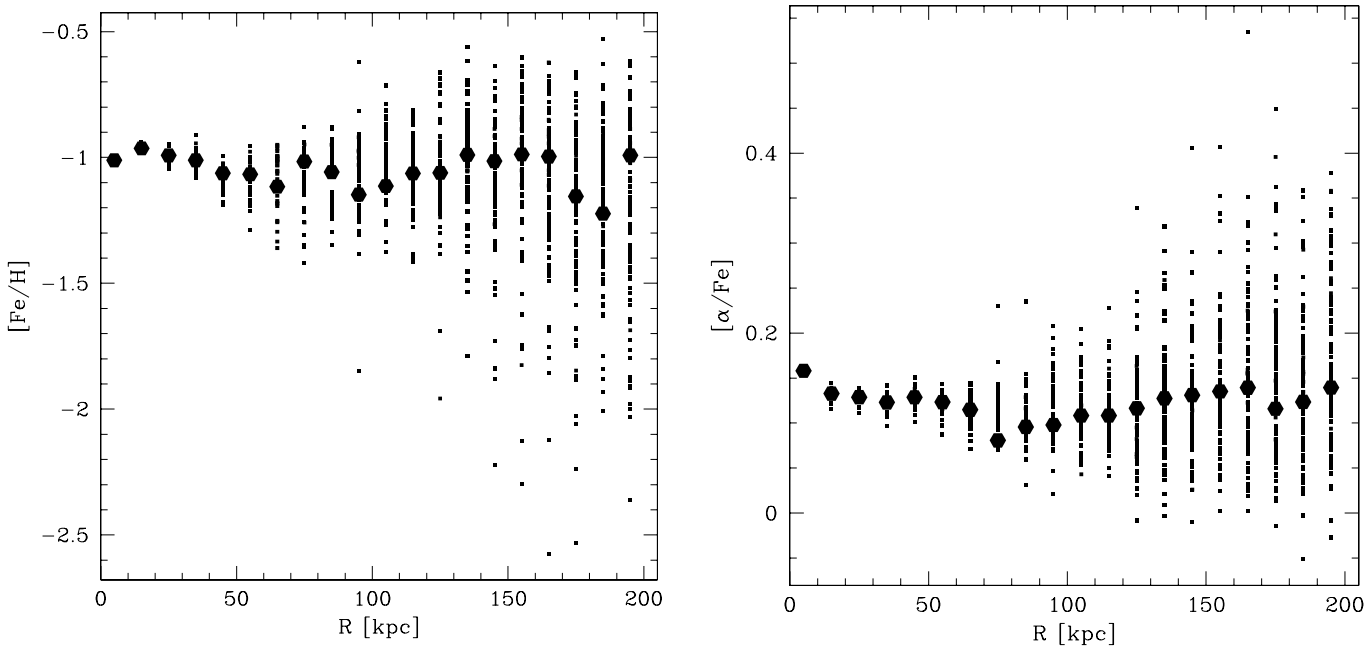

FIG. 12.—The [Fe/H] (*left*) and [α/Fe] (*right*) distributions vs. cylindrical radius R in Halo H1, [$R = (x^2 + z^2)^{1/2}$]. Large pentagons correspond to weight-averaged [Fe/H] or [α/Fe] values in cylindrical shells of width $dR = 10$ kpc. Small squares correspond to weight-averaged [Fe/H] or [α/Fe] values at equidistant azimuthal angles $\phi \in [0,\ 2\pi]$ in a given cylindrical shell. (Note that the number of angles ϕ probed in each shell increases with R so as to preserve the size of the mock observational fields.)

Our results suggest that metallicity gradients of less than 1 dex over distances of a few tens of kiloparsecs are consistent with the hierarchical structure formation scenario. However, for a more accurate comparison between our models and observations, we have to take into account the methods of measurement used in observations. For example, in external galaxies radial distances cannot be currently determined. What observations generally measure are the separations from the centers of galaxies, which are projected radii on the plane of the sky. Moreover, current observations probe small fields in the stellar halos at different projected radii (e.g., Bellazzini et al. 2003). We illustrate this with a mock observation of one of our halos (H1). Figure 12 shows the [Fe/H] and [α/Fe] distributions versus the projected radius R on the plane (x, z). The large symbols are averages in cylindrical shells, while the small symbols show the decomposition of these values at equidistant azimuthal angles in each cylindrical shell. Thus, each small symbol approximates a projected field of observation a few kiloparsecs on a side, similar to the size of observational fields. Figure 12 demonstrates that a large spread in either [Fe/H] or [α/Fe] may exist at a given R, and therefore, a random sampling with small fields over different projected radii can result in a detection of spurious abundance gradients. Our results therefore caution that a wider spatial sampling of halos is necessary in order to confirm the current detections of abundance gradients.

5. CONCLUSIONS

The motivation of this work was to provide predictions of the hierarchical formation paradigm that can be tested with the data from current and upcoming astrometric and spectroscopic observations. In this study we have explored the global properties as the phase-space distribution of the [Fe/H] and [α/Fe] chemical abundances in a series of Milky Way–type stellar halos formed in a ΛCDM universe. Our results are summarized below.

1. For a fixed dark matter halo mass, we predict that stellar halo metallicities increase with stellar halo mass. The resulting [Fe/H]-M_* relation for stellar halos arises because high-mass stellar halos tend to have accreted a larger number of metal-rich satellite progenitors (more massive and/or accreted at later times).

2. Chemical abundance distributions provide important links to the merger histories of galaxies. For example, the metallicity differences between the metal-poor halos in our sample ([Fe/H] $\simeq -1.3$) and the most metal-rich ones ([Fe/H] $\simeq -0.9$) can be explained by the larger number of massive (metal-rich) satellite accretions in the latter case. This result suggests that the observed metallicity differences between the (metal-poor) Milky Way and the (metal-rich) M31 may arise because M31 destroyed one or two more massive satellites than the Milky Way.

3. In agreement with observations, we find that all simulated halos contain an underlying population of old metal-poor stars. More massive halos contain additional intermediate-age populations accreted more recently.

4. In contrast with the Milky Way, some of our halo models contain old stellar populations that are metal-rich, originating in massive satellites ($M_* \sim 10^9\ M_\odot$) accreted early on. The metallicity constraints seems to suggest that the Milky Way has an atypical mass accretion history, lacking in massive early accretion events, when compared with other galaxies of a similar mass.

5. We predict metallicity gradients in [Fe/H] and [α/Fe] in our *hierarchically formed* stellar halos that are often non-negligible. Gradients extend typically over a few tens of kiloparsecs and may be as large as 0.5 dex in [Fe/H] and 0.2 dex in [α/Fe]. Thus, evidence for metallicity gradients alone in the Milky Way stellar halo would not preclude its formation via a hierarchical process. Only coupled with phase-space data can metallicity information be used to test ideas about accreted versus in situ formation.

6. We predict that most metal-poor stars in the Galactic halo are buried within the central $\sim$5 kpc of the Galaxy. This will likely be important for efforts to use the observed count of low-metallicity stars to constrain models of cosmic reionization and the transition from Population III to Population II star formation (e.g., Tumlinson et al. 2004).

7. We suggested a method for identifying cold tidal streams in stellar halos by selecting stars with $[\alpha/\mathrm{Fe}] \leq 0.05$, which trace streams from recently accreted satellites. If used to complement the common kinematical identification methods, the proposed selection criterion may improve the detection of tidal streams.

Combining kinematic and chemical abundance information proves to be a powerful tool for understanding how galaxies form and evolve. In anticipation to the wealth of data to be delivered by current and future Galactic surveys, it is important to develop and improve on numerical simulations of the chemical evolution of the Galaxy in a realistic cosmological context, such as those presented in our study, and to devise criteria to identify more tidal streams.

While our methods successfully reproduce the gross chemical abundance properties of the Galactic halo and satellite dwarf galaxies, our treatments of dissipational physics including star formation, gas cooling, and energetic feedback mechanisms may be too simplistic to recover the detailed properties of the modeled systems with high accuracy. For instance, the assumed truncation of star formation in dwarf systems after they accrete into their host galaxy is very approximate. Gravitational torques applied by the central galaxy and other satellite systems may induce episodes of efficient star formation in the dwarfs we model, especially near-pericentric passage. Such bursts occurred in the LMC and SMC, as inferred from their stellar populations (e.g., Smecker-Hane et al. 2002; Harris & Zaritsky 2004), and should be modeled if more accurate chemical enrichment histories for dwarf systems are to be achieved.

These complications speak to the need for high-resolution hydrodynamical simulations of the formation of the Galactic stellar halo and dwarf satellite population. While recent hydrodynamical simulations have begun to address this issue (e.g., Brook et al. 2004), they have not yet matched the mass resolution necessary to capture the entire population of dwarfs galaxies we follow in our collisionless simulations nor the full complexity of our chemical enrichment model. We acknowledge the importance of the previous work and look forward to increasingly sophisticated hydrodynamical simulations of the cosmological formation of the Galactic stellar halo.

The authors wish to thank Annette Ferguson, Tom Brown, Harry Ferguson, Raja Guhathakurta, and Chris Purcell for helpful discussions. A. F. and K. V. J.'s contributions were supported through NASA grant NAG5-9064 and NSF career award AST-0133617. J. S. B. is supported by the Center for Cosmology at University of California, Irvine.

REFERENCES

Abadi, M. G., Navarro, J. F., & Steinmetz, M. 2006, MNRAS, 365, 747
Altmann, M., Catelan, M., & Zoccali, M. 2005, A&A, 439, L5
Beers, T. C., et al. 2005, in IAU Symp. 228, From Lithium to Uranium: Elemental Tracers of Early Cosmic Evolution, ed. V. Hill, P. Francois, & F. Primas (Cambridge: IAU), 175
Bekki, K., & Chiba, M. 2001, ApJ, 558, 666
Bellazzini, M., Cacciari, C., Federici, L., Fusi Pecci, F., & Rich, M. 2003, A&A, 405, 867
Blumenthal, G. R., Faber, S. M., Primack, J. R., & Rees, M. J. 1984, Nature, 311, 517
Brook, C. B., Kawata, D., Gibson, B. K., & Flynn, C. 2003, ApJ, 585, L125
———. 2004, MNRAS, 349, 52
Brown, T. M., et al. 2003, ApJ, 592, L17
Bullock, J. S., & Johnston, K. V. 2005, ApJ, 635, 931
Bullock, J. S., Kravtsov, A. V., & Weinberg, D. H. 2001, ApJ, 548, 33
Carney, B. W., Laird, J. B., Latham, D. W., & Aguilar, L. A. 1996, AJ, 112, 668
Chiba, M., & Beers, T. C. 2000, AJ, 119, 2843
Dekel, A., & Silk, J. 1986, ApJ, 303, 39
Dekel, A., & Woo, J. 2003, MNRAS, 344, 1131
Diemand, J., Madau, P., & Moore, B. 2005, MNRAS, 364, 367
Dinescu, D. I. 2002, in ASP Conf. Ser. 265, Omega Centauri: A Unique Window into Astrophysics, ed. F. van Leeuwen, J. D. Hughes, & G. Piotto (San Fransisco: ASP), 365
Eggen, O. J., Lynden-Bell, D., & Sandage, A. R. 1962, ApJ, 136, 748 (ELS62)
Fardal, M. A., Babul, A., Geehan, J. J., & Guhathakurta, P. 2006, MNRAS, 366, 1012
Ferguson, A. M. N., Irwin, M. J., Ibata, R. A., Lewis, G. F., & Tanvir, N. R. 2002, AJ, 124, 1452
Ferguson, A. M. N., et al. 2005, ApJ, 622, L109
Font, A. S., Johnston, K. V., Bullock, J. S., & Robertson, B. E. 2006a, ApJ, 638, 585
Font, A. S., Johnston, K. V., Guhathakurta, P., Majewski, S. R., & Rich, R. M. 2006b, AJ, 131, 1436
Freeman, K., & Bland-Hawthorn, J. 2002, ARA&A, 40, 487
Gallazzi, A., et al. 2005, MNRAS, 362, 41
Gilbert, K. M., et al. 2006, ApJ, submitted (astro-ph/0605171)
Guhathakurta, P., et al. 2006a, AJ, 131, 2497
———. 2006b, ApJ, submitted (astro-ph/0605172)
Hargis, J. R., Sandquist, E L., & Bolte, M. 2004, ApJ, 608, 243
Harris, G. L. H., Harris, W. E., & Poole, G. B. 1999, AJ, 117, 855
Harris, J., & Zaritsky, D. 2004, AJ, 127, 1531
Harris, W. E., & Harris, G. L. H. 2002, AJ, 123, 3108
Helmi, A., & de Zeeuw, P. T. 2000, MNRAS, 319, 657
Helmi, A., Navarro, J. F., Nordström, B., Holmberg, J., Abadi, M. G., & Steinmetz, M. 2006, MNRAS, 365, 1309
Helmi, A., White, S. D. M., de Zeeuw, P. T., & Zhao, H. 1999, Nature, 402, 53
Helmi, A., White, S. D. M., & Springel, V. 2003, MNRAS, 339, 834
Ibata, R. A., Chapman, S., Ferguson, A. M. N., Irwin, M., Lewis, G. F., & McConnachie, A. 2004, MNRAS, 351, 117
Ibata, R., Chapman, S., Ferguson, A. M. N., Lewis, G., Irwin, M., Tanvir, N. 2005, ApJ, 634, 287
Ibata, R. A., Irwin, M. J., Ferguson, A. M. N., Lewis, G. F., & Tanvir, N. 2001, Nature, 412, 49
Irwin, M., Ferguson, A. M. N., Ibata, R., Lewis, G., & Tanvir, N. 2005, ApJ, 628, L105
Johnston, K. V. 1998, ApJ, 495, 297
Kalirai, J. S., et al. 2006, ApJ, 641, 268
Kauffmann, G., Colberg, J. M., Diaferio, A., & White, S. D. M. 1999, MNRAS, 303, 188
Knebe, A., Gill, S. P. D., Kawata, D., & Gibson, B. K. 2005, MNRAS, 357, L35
Laird, J. B., Carney, B. W., Rupen, M. P., & Latham, D. W. 1988, AJ, 96, 1908
Larson, R. B. 1974, MNRAS, 169, 229
Majewski, S. R., Munn, J. A., & Hawley, S. L. 1996, ApJ, 459, L73
Mayer, L., Moore, B., Quinn, T., Governato, F., & Stadel, J. 2002, MNRAS, 336, 119
Moore, B., Diemand, J., Madau, P., Zemp, M., & Stadel, J. 2006, MNRAS, 368, 563
Mouhcine, M., Ferguson, H. C., Rich, R. M., Brown, T. M., & Smith, T. E. 2005a, ApJ, 633, 821
———. 2005b, ApJ, 633, 828
Navarro, J. F., Helmi, A., & Freeman, K. C. 2004, ApJ, 601, L43
Nissen, P. E., & Schuster, W. J. 1991, A&A, 251, 457
———. 1997, A&A, 326, 751
Perryman, M. A. C., et al. 2001, A&A, 369, 339
Reitzel, D. B., & Guhathakurta, P. 2002, AJ, 124, 234
Renda, A., et al. 2005, MNRAS, 363, L16
Robertson, B., Bullock, J. S., Font, A. S., Johnston, K. V., & Hernquist, L. 2005, ApJ, 632, 872
Searle, L. 1977, in The Evolution of Galaxies and Stellar Populations, ed. B. M. Tinsley & R. B. Larson (New Haven: Yale Univ. Press), 219
Searle, L., & Zinn, R. 1978, ApJ, 225, 357 (SZ78)
Smecker-Hane, T. A., Cole, A. A., Gallagher, J. S., & Stetson, P. B. 2002, ApJ, 566, 239
Springel, V., White, S. D. M., Tormen, G., & Kauffmann, G. 2001, MNRAS, 328, 726
Steinmetz, M. 2003, in ASP Conf. Ser. 298, GAIA Spectroscopy: Science and Technology, ed. U. Munari (San Fransisco: ASP), 381
Tinsley, B. M. 1980, Fundam. Cosm. Phys., 5, 287
Tumlinson, J., Venkatesan, A., & Shull, J. M. 2004, ApJ, 612, 602

White, S. D. M., & Rees, M. 1978, MNRAS, 183, 341
White, S. D. M., & Springel, V. 2000, in The First Stars Workshop Proceedings, ed. A. Weiss, T. G. Abel, & V. Hill (Berlin: Springer), 327
Wyse, R. F. G. 2001, in ASP Conf. Ser. 230, Galactic Disks and Disk Galaxies, ed. J. Funes & E. Corsini (San Francisco: ASP), 71
Zentner, A. R., & Bullock, J. S. 2003, ApJ, 598, 49
Zibetti, S., White, S. D. M., & Brinkmann, J. 2004, MNRAS, 347, 556
Zinn, R. 1993, in ASP Conf. Ser. 48, The Globular Clusters-Galaxy Connection, ed, G. H. Smith & J. P. Brodie (San Fransisco: ASP), 38